J Nanostruct 16(2): 2467-2483, Spring 2026

RESEARCH PAPER

Preparation and Evaluation of Curcumin-Loaded Selenium Nanoparticles Coated with Chitosan Against Staphylococcus Aureus and Pseudomonas Aeruginosa, and Assessment of Biofilm and FtsZ Protein Gene Expression

Hedayat Jalali [1], Abolfazl Gholipour [1], Dhiya Altememy [2], Pegah Khosraviyan [3], Mansoor Khaledi [1], Behnam Poureslamfar [4], Behnam Zamanzad [1], Fatemeh Banisharif [1], Milad Shahini Shams Abadi [3] *

[1] *Cellular and Molecular Research Center, Basic Health Sciences Institute, Shahrekord University of Medical Sciences, Shahrekord, Iran*

[2] *Department of Pharmaceutics, College of Pharmacy, Al-Zahraa University for Women, Karbala, Iraq*

[3] *Medical Plants Research Center, Basic Health Sciences Institute, Shahrekord University of Medical Sciences, Shahrekord, Iran*

[4] *Department of Biology, Faculty of Science, Yasouj University, Yasouj, Iran*

ARTICLE INFO

Article History:
Received 09 January 2026
Accepted 27 March 2026
Published 01 April 2026

Keywords:
Anti-biofilm
Antibacterial activity
Curcumin
Selenium nanoparticles
Staphylococcus aureus
Pseudomonas aeruginosa

ABSTRACT

An alarming agent for global health systems is emerging against antibiotic resistance, due in particular to *S. aureus* and *P. aeruginosa*. Thus, it becomes an emergency to design novel antimicrobial interventions. Selenium nanoparticles (SeNPs) loaded with curcumin and coated with chitosan (CS-Cur-SeNPs) might be an appropriate candidate due to their biocompatibility and proven efficacy in inhibiting bacteria and biofilm formation. Accordingly, in this study, the antibacterial and antibiofilm potentials of CS-Cur-SeNPs were investigated against the expression of critical virulent genes (icaD, lasI, and ftsZ). The synthesis of SeNPs, Cur-SeNPs, and CS-Cur-SeNPs was done, and characterization followed using dynamic light scattering (DLS), scanning electron microscopy (SEM), and FTIR spectroscopy methods. Antibacterial assays by disk diffusion and MIC were carried out against *S. aureus* (ATCC 25923) and *P. aeruginosa* (ATCC 27853) with the samples synthesized. Anti-biofilm activity was also checked using crystal violet staining. The mRNA expression of icaD, lasI, and ftsZ was studied by means of qRT. CS-Cur-SeNPs exhibited superior antibacterial activity, with inhibition zones of 20 ± 2 mm (*S. aureus*) and 17 ± 2 mm (*P. aeruginosa*), and MICs of 8 µg/mL (*S. aureus*) and 16 µg/mL (*P. aeruginosa*), compared to SeNPs and Cur-SeNPs ($p < 0.05$). Biofilm inhibition reached 85 ± 7% for *S. aureus* and 75 ± 6% for *P. aeruginosa* at MIC concentrations ($p < 0.001$). qRT-PCR revealed significant downregulation of *icaD* (3.2-fold) and *ftsZ* (2.8-fold) in *S. aureus*, and *lasI* (2.5-fold) and *ftsZ* (2.3-fold) in *P. aeruginosa* ($p < 0.05$). TEM and FTIR confirmed the spherical morphology and successful coating of CS-Cur-SeNPs. CS-Cur-SeNPs provide an anti-bacterial and anti-biofilm activity against *S. aureus* and *P. aeruginosa*, disrupting growth in vitro, the formation of biofilms, and the expression of virulence genes. Hence, with enhanced in vivo and clinical studies, this may serve as a novel therapeutic strategy for fighting antibiotic-resistant infections.

How to cite this article
Jalali H., Gholipour A., Altememy D. et al. Preparation and Evaluation of Curcumin-Loaded Selenium Nanoparticles Coated with Chitosan Against Staphylococcus Aureus and Pseudomonas Aeruginosa, and Assessment of Biofilm and FtsZ Protein Gene Expression. J Nanostruct, 2026; 16(2):2467-2483. DOI: 10.22052/JNS.2026.02.087

* *Corresponding Author Email: Shahini_milad@yahoo.com*

INTRODUCTION

Antimicrobial resistance caused an estimated 4.95 million deaths worldwide in 2019, highlighting the urgent need for global action [1]. With multi-drug-resistant bacterial pathogens such as *Staphylococcus aureus* and *Pseudomonas aeruginosa*, there is an urgent need for new treatments to treat infections that evade conventional ones [2]. Preparing selenium nanoparticles loaded with curcumin and coated with chitosan provides an enticing strategy of overcoming bacterial resistance by impeding bacterial growth and biofilm formation, as well as their cell division.

Staphylococcus aureus, identified as a gram-positive coccus, is a versatile pathogen that causes infections from abscesses on the skin to life-threatening bacteremia and endocarditis [3]. It can form biofilms with the help of the icaD gene, and attrition of its Exotoxins causes the pathogen to become virulent while resisting antibiotics [4, 5]. In contrast, *Pseudomonas aeruginosa* is a tetra-shaped bacillus and is among the highly reported hospital infections in immunocompromised patients [6]. Its mechanisms of evading treatments, in essence, efflux pumps and beta-lactamases, are quite successful, coupled with biofilm formation via genes like lasI. This has led to lethargic, full-blown killing, with MDR strains being linked to a 79 percent rate of death in grave cases [7, 8].

The FtsZ protein for bacterial cell division is essential for the survival of both pathogens, as it forms a Z-ring responsible for cytokinesis [9]. When FtsZ is inhibited, bacterial growth is impaired, thereby presenting itself as a very attractive target for novel antimicrobials [10]. Nanotechnology further brings very special properties to this approach through nanoparticles, such as having a high surface-to-volume ratio and enhanced drug delivery [11]. Selenium nanoparticles are also very low in toxicity, with inherent antibacterial potential that works against cell membrane formation and inhibits biofilm formation [12, 13]. Curcumin is a polyphenol derived from turmeric, which presents antimicrobial and anti-biofilm features but suffers from limited solubility and bioavailability [14, 15]. Chitosan is biocompatible and allows improving the stability of nanoparticles with pH-dependent drug release for aiding bacterial cell targeting [16, 17].

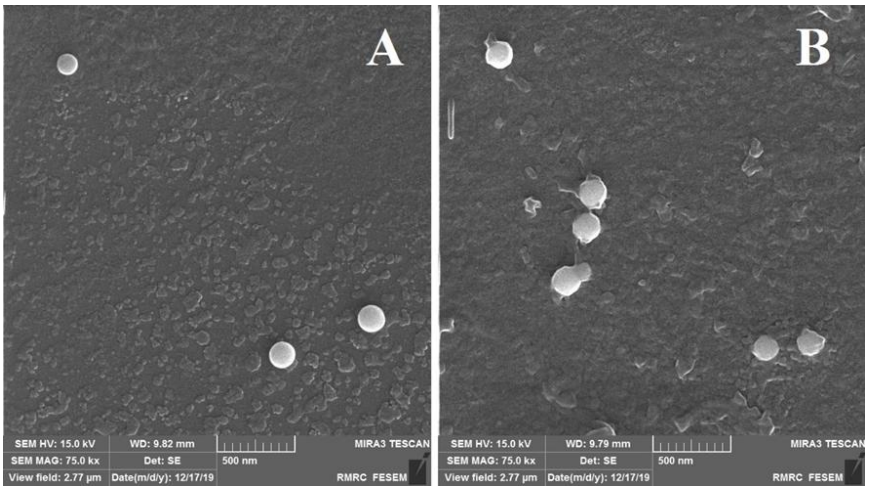

Fig. 1. SEM images of selenium nanoparticles (A) and chitosan-coated selenium nanoparticles (B).

Table 1. Primers Used for qRT-PCR Analysis.

Gene	Forward Primer (5'-3')	Reverse Primer (5'-3')	Reference
icaD	ATGGTCAAAGCCCAGACAGA	CGTGTTTTCAACATTTAATGCAA	[5]
lasI	CGCTGGAACTGGATGAAGTT	GCTCTTGGATTCGGGTGTTA	[8]
ftsZ	GTGATTGACCGTCTTGGTGA	TCTTCACCAACAGCGAAACC	[26]
16S rRNA	GGAATTCCATGTGTAGCGGTG	TCCCCGTAGACCTCATCGTTT	[7]

Conflicting results in the literature show the need for further research. It is stated that some researchers have lagged in demonstrating the strong antibacterial effect of SeNPs and curcumin against *S. aureus*, whereas other researchers suggested that their antibacterial effect on *P. aeruginosa* is variable, probably due to changes in the cell wall structure [18]. The use of these components is based on the rationale that incorporation of SeNPs, curcumin, and chitosan would work synergistically in promoting antimicrobial and anti-biofilm activity. Completely relevant molecular interaction studies and their long-term safety are still missing.

The current study evaluated the acute anti-biofilm and antibacterial effect of curcumin-based functionalized SeNPs coated with chitosan against methicillin-resistant *Staphylococcus aureus* (MRSA) and *Pseudomonas aeruginosa* (PAO), and especially on the expression of icaD, lasI, and ftsZ genes. This research gap is to be filled to contribute to the future acquisition of new pharmaceutical solutions applied to multidrug-resistant (MDR) bacterial infections.

MATERIALS AND METHODS

Bacterial Strains and Culture Conditions

The study utilized *Staphylococcus aureus* (ATCC 25923) and *Pseudomonas aeruginosa* (ATCC 27853) as standard strains, obtained from the

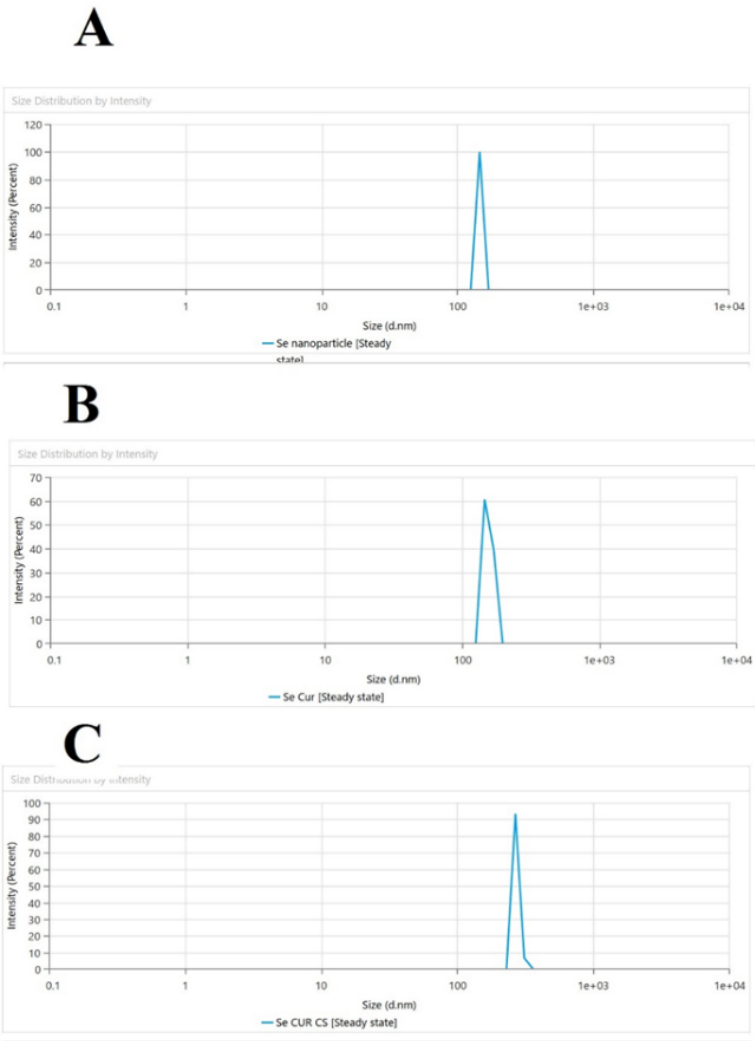

Fig. 2. Size of selenium nanoparticles (A), selenium-curcumin (B), and selenium-curcumin-chitosan (C) using DLS.

Pasteur Institute of Iran. Both strains were cultured in Luria-Bertani (LB) broth at 37°C with shaking at 200 rpm for 24 hours. Bacterial suspensions were adjusted to a turbidity equivalent to 0.5 McFarland standard (approximately 1.5×10^8 CFU/mL) using a spectrophotometer at 600 nm for subsequent experiments [19].

Preparation of Selenium Nanoparticles (SeNPs) Loaded with Curcumin and Coated with Chitosan

Selenium nanoparticles (SeNPs) were synthesized via a chemical reduction method as described by Menon et al. (2020) [20]. Sodium selenite (Na_2SeO_3, 5 mM) was reduced with ascorbic acid (10 mM) in a 1:4 molar ratio under constant stirring at room temperature for 2 hours. Curcumin (10 mg/mL) was dissolved in ethanol and mixed with the SeNP solution at a 1:10 ratio, followed by sonication for 30 minutes to ensure uniform loading. Chitosan (0.5% w/v, medium molecular weight, 85% deacetylated) was dissolved in 1% acetic acid and added dropwise to the curcumin-loaded SeNP solution under stirring at 1000 rpm for 1 hour to achieve coating. The resulting nanoparticles were centrifuged at 12,000 rpm for 20 minutes, washed with distilled water, and lyophilized for further use. Nanoparticle characterization was performed using dynamic light scattering (DLS) for size and zeta potential, transmission electron microscopy (TEM) for morphology, and Fourier-transform infrared spectroscopy (FTIR) for chemical composition [21].

Antibacterial Activity Assessment

The antibacterial activity of SeNPs, curcumin-loaded SeNPs (Cur-SeNPs), and chitosan-coated Cur-SeNPs (CS-Cur-SeNPs) was evaluated using the disk diffusion method and minimum inhibitory concentration (MIC) assay. For the disk diffusion method, 100 µL of bacterial suspension (0.5 McFarland) was spread on Mueller-Hinton agar plates. Sterile paper disks (6 mm diameter) impregnated with 20 µL of nanoparticle suspensions (50 µg/mL) were placed on the agar surface. Plates were incubated at 37°C for 24 hours, and the diameter of inhibition zones was measured in millimeters [22]. The MIC was determined using a broth microdilution assay in 96-well plates, with nanoparticle concentrations ranging from 0.5 to 256 µg/mL. After incubation at 37°C for 24 hours, the lowest concentration preventing visible bacterial growth was recorded as the MIC [23].

Anti-Biofilm Activity Assessment

Biofilm formation was assessed using the crystal violet staining method in 96-well polystyrene plates. Bacterial suspensions (100

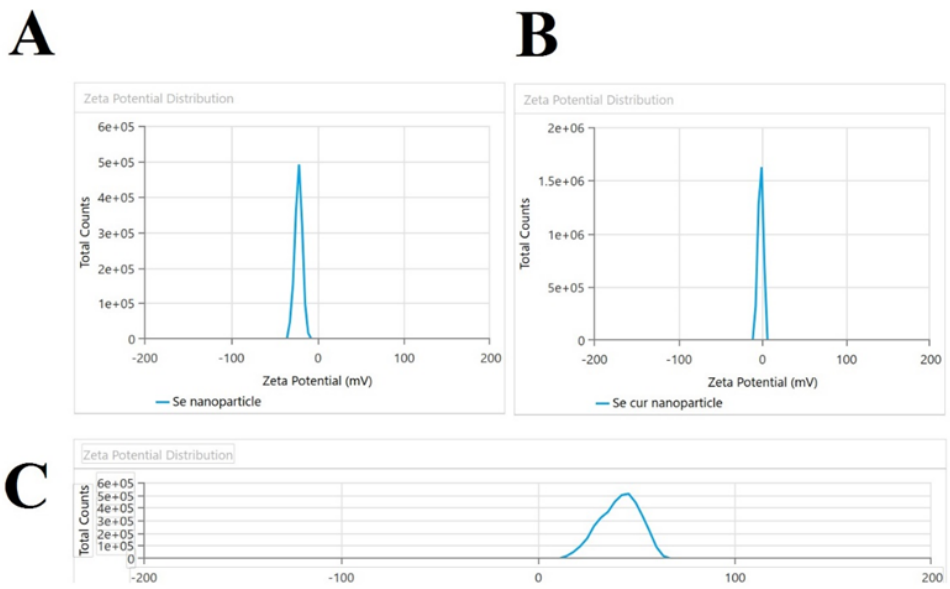

Fig. 3. Zeta potential of selenium nanoparticles (A), selenium-curcumin (B), and selenium-curcumin-chitosan (C) using DLS.

µL, 0.5 McFarland) were incubated with varying concentrations of CS-Cur-SeNPs (0.5 × MIC to 2 × MIC) at 37°C for 48 hours. After incubation, plates were washed with phosphate-buffered saline (PBS) to remove planktonic cells, and biofilms were stained with 0.1% crystal violet for 15 minutes. Excess dye was washed off, and the bound dye was solubilized with 95% ethanol. Absorbance was measured at 595 nm using a microplate reader to quantify biofilm biomass. Percentage inhibition was calculated relative to untreated controls [24].

Gene Expression Analysis

The expression levels of *icaD* (*S. aureus*), *lasI* (*P. aeruginosa*), and *ftsZ* (both strains) were analyzed using quantitative real-time PCR (qRT-PCR). Bacterial cells were treated with CS-Cur-SeNPs at sub-MIC concentrations for 24 hours. Total RNA was extracted using a commercial RNA extraction kit, and cDNA was synthesized using a reverse transcription kit. qRT-PCR was performed with SYBR Green master mix on a Bio-Rad CFX96 system. Primers for *icaD*, *lasI*, and *ftsZ* were designed based on sequences from the NCBI database (Table 1). Relative gene expression was calculated using the $2^{-}\Delta\Delta Ct$ method, normalized to the 16S rRNA housekeeping gene [25].

Statistical Analysis

Data were analyzed using SPSS version 22.0 (IBM, USA). Normality was assessed with the Kolmogorov-Smirnov test. Differences in

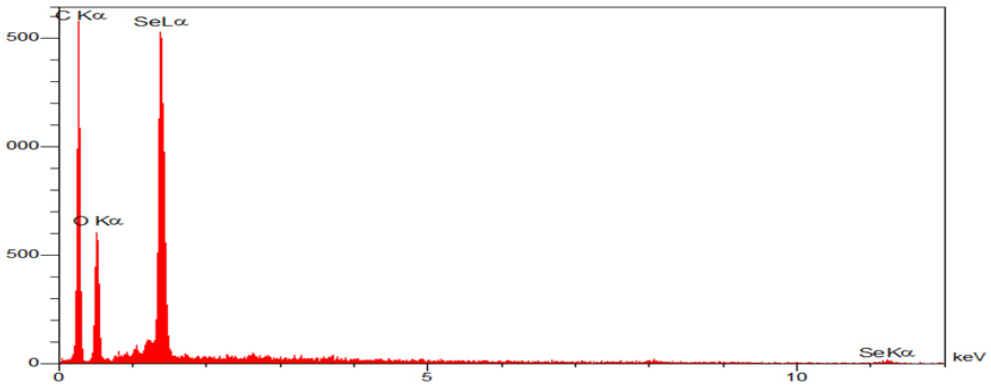

Fig. 4: EDAX Analysis of Elemental Composition of Nanoparticles. A) Selenium, B) Selenium/Curcumin, C) Selenium/Curcumin/Chitosan.

Table 2. EDAX Analysis of Selenium, Curcumin, and Chitosan Nanoparticles.

Element	SeNPs (%W)	Se+Cur (%W)	Se+Cur+CS (%W)
C	0	45.94	37.13
N	0	0	0.45
O	21.52	19.35	11.52
Se	78.48	34.71	50.90

Table 3. Loading Efficiency and Loading Capacity of Selenium-Curcumin and Selenium-Curcumin-Chitosan Nanoparticles.

Nanoparticles	Loading Capacity (%)	Loading Efficiency (%)
Se-Cur	56.2 ± 4.85	97 ± 1.1
Se-Cur-Cs	53.88 ± 8.6	99.3 ± 0.2

inhibition zones, MIC values, and biofilm inhibition percentages between treatment groups and controls were evaluated using one-way ANOVA followed by Tukey's post-hoc test. Gene expression data were analyzed using the Student's t-test to compare treated and untreated groups. Results were expressed as mean ± standard deviation (SD), and a p-value < 0.05 was considered statistically significant [27].

RESULTS AND DISCUSSION

Nanoparticle Characterization

Morphological Characterization

The surface morphology and characteristics of selenium nanoparticles (SeNPs) and chitosan-coated selenium nanoparticles (CS-SeNPs) were evaluated using scanning electron microscopy (SEM). The images confirmed spherical, uniformly distributed particles with sizes ranging from 100–150 nm for SeNPs and 150–250 nm for CS-SeNPs, with a visible halo confirming the chitosan coating [21]. SEM images showing spherical SeNPs (A) and CS-SeNPs (B) with a distinct chitosan coating halo. Scale bar: 200 nm.

Particle Size and Zeta Potential Analysis

Dynamic light scattering (DLS) was employed to measure the hydrodynamic size of SeNPs, curcumin-loaded SeNPs (Cur-SeNPs), and chitosan-coated curcumin-loaded SeNPs (CS-Cur-SeNPs). The sizes were 146.1 nm, 155.5 nm, and 270 nm, respectively, reflecting the sequential addition of coating layers [21]. Zeta potential measurements revealed values of -21.59 mV for SeNPs, -1.755 mV for Cur-SeNPs (attributed to curcumin's secondary amine groups), and +41.66 mV for CS-Cur-SeNPs (due to chitosan's amino groups) [27].

Bar chart displaying particle sizes of SeNPs (146.1 nm), Cur-SeNPs (155.5 nm), and CS-Cur-SeNPs (270 nm).

Bar chart showing zeta potentials of SeNPs (-21.59 mV), Cur-SeNPs (-1.755 mV), and CS-Cur-SeNPs (+41.66 mV).

Elemental Composition Analysis

Energy-dispersive X-ray (EDAX) analysis confirmed the presence of carbon, oxygen, selenium, and nitrogen in SeNPs, Cur-SeNPs, and CS-Cur-SeNPs. SeNPs exhibited higher selenium and oxygen content, while Cur-SeNPs and CS-Cur-SeNPs showed increased carbon and nitrogen percentages, confirming curcumin and chitosan coatings [28]. EDAX spectra displaying a prominent selenium peak at ~1.5 keV and a weaker peak at ~11 keV, with carbon, oxygen, and nitrogen peaks at 0.5–0.7 keV.

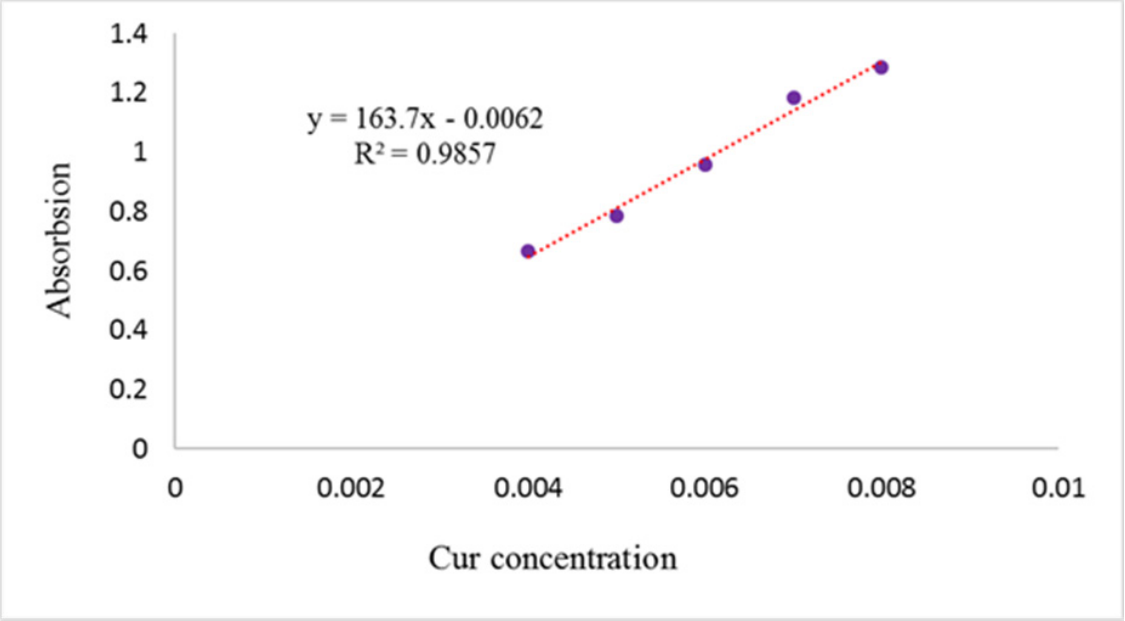

Fig. 5. Curcumin Calibration Curve.

Curcumin Loading and Efficiency

Curcumin loading capacity and efficiency were determined using a calibration curve (y = 163.7x - 0.0062) with concentrations ranging from 4 to 8 µg/mL and absorbance from 0.668 to 1.286 [29]. Loading capacity and efficiency were calculated for Cur-SeNPs and CS-Cur-SeNPs. Calibration curve for curcumin with equation y = 163.7x - 0.0062, $R^2 \approx 0.99$.

Curcumin Release Profile

The release of curcumin from CS-Cur-SeNPs was evaluated in vitro at pH 5 and 7.4. Release was gradual and controlled at pH 5, with chitosan's polymeric network reducing release intensity at pH 7.4 due to enhanced electrostatic interactions [29]. Line chart illustrating controlled curcumin release from CS-Cur-SeNPs at pH 5 compared to pH 7.4.

Antibacterial Activity

Minimum inhibitory concentrations (MICs) were determined using broth microdilution for *Staphylococcus aureus* (ATCC 25923) and

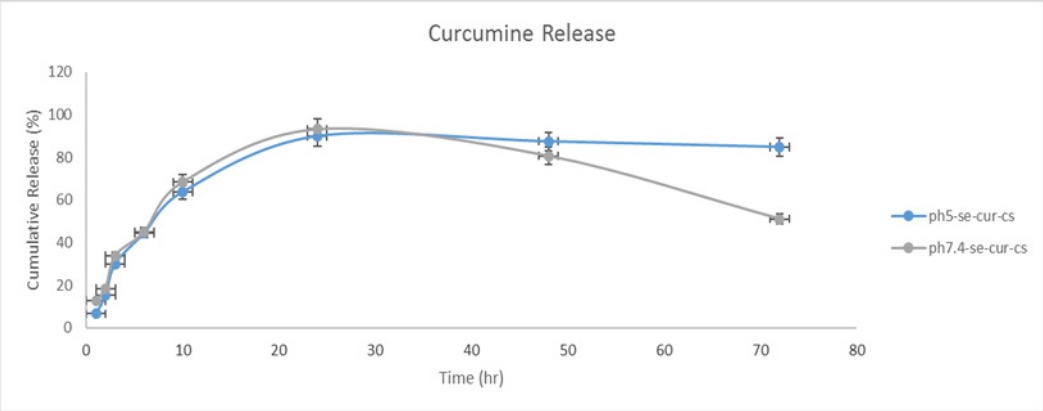

Fig. 6. Evaluation of Curcumin Release from Selenium Nanoparticles.

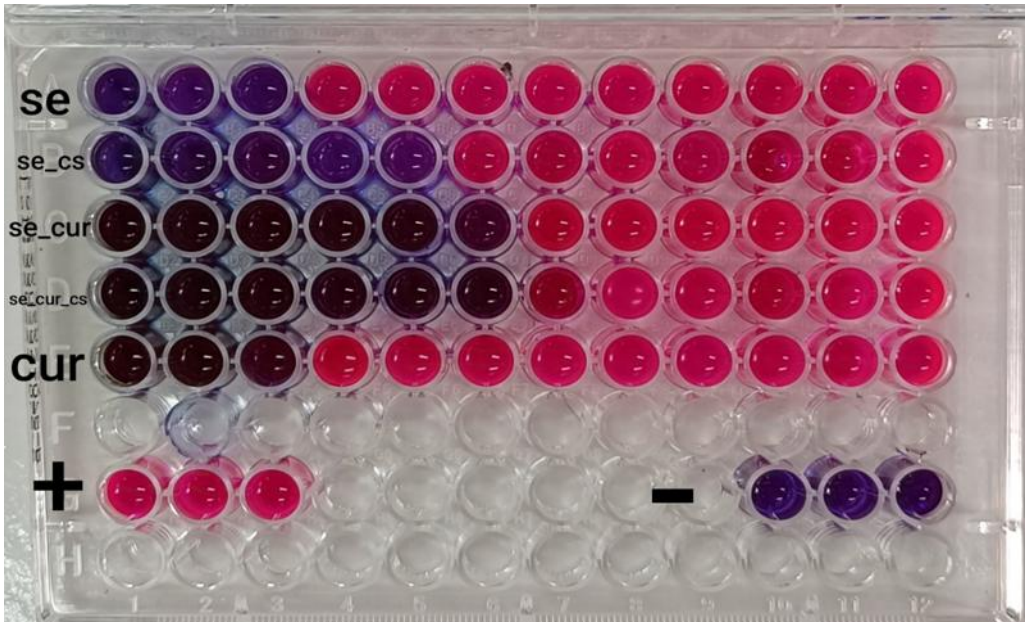

Fig. 7. MIC Test (Original Image).

Pseudomonas aeruginosa (ATCC 27853), with experiments performed in triplicate [30]. CS-Cur-SeNPs exhibited the lowest MICs, demonstrating superior antibacterial activity, particularly against *S. aureus* [22, 31]. Fig. 7 shows MIC results for *S. aureus* with clear wells at 0.125 mg/mL (SeNPs), 0.0312 mg/mL (CS-SeNPs), 0.0156 mg/mL (Cur-SeNPs and CS-Cur-SeNPs), and 0.125 mg/mL (curcumin). Fig. 8 shows MIC results for *P. aeruginosa* with clear wells at 0.25 mg/mL

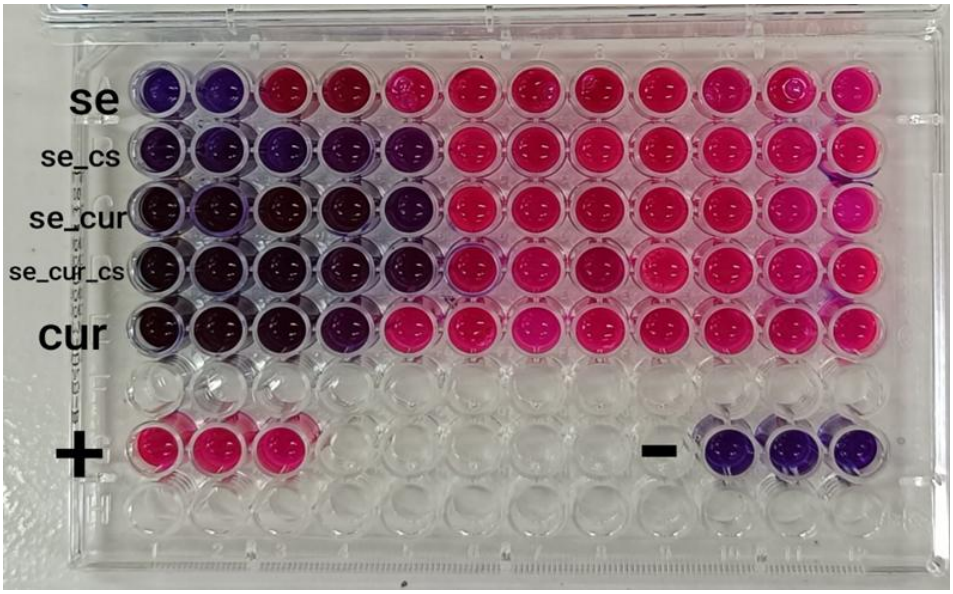

Fig. 8. MIC Test (Original Image).

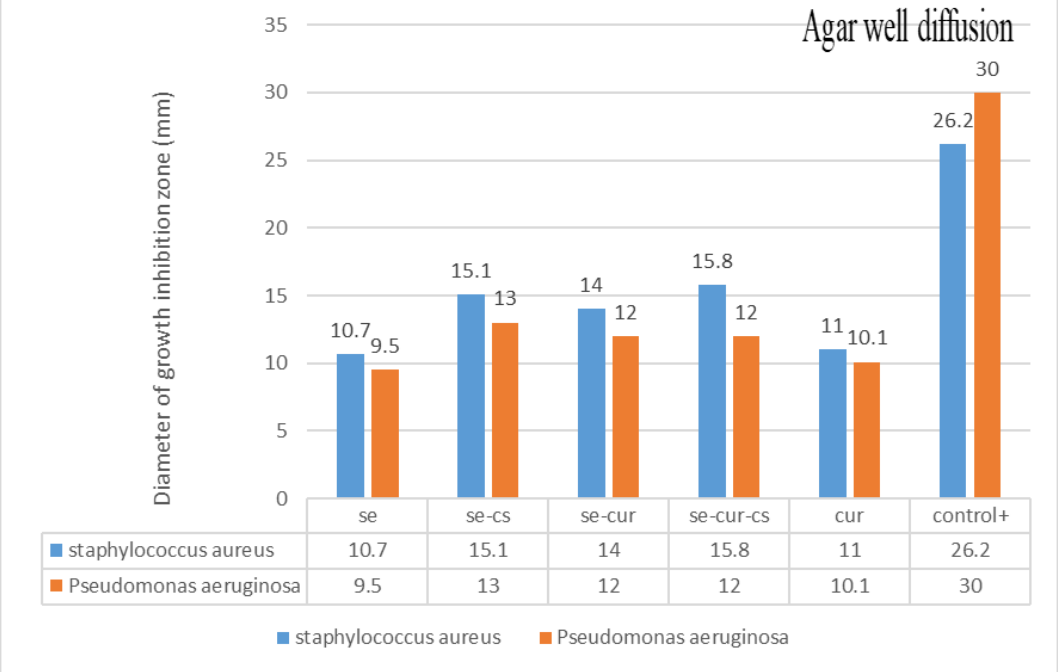

Fig. 9. Agar Well Diffusion Test.

(SeNPs), 0.0312 mg/mL (CS-SeNPs, Cur-SeNPs, CS-Cur-SeNPs), and 0.0625 mg/mL (curcumin).

Bar chart comparing inhibition zone diameters for S. aureus and P. aeruginosa treated with nanoparticles versus antibiotics (vancomycin for S. aureus, imipenem for P. aeruginosa) (Fig. 9).

Image showing inhibition zones for S. aureus with diameters of 11 mm (vancomycin), 15.8 mm (SeNPs), 14 mm (CS-SeNPs), 15.1 mm (Cur-SeNPs), 10.7 mm (CS-Cur-SeNPs), and 26 mm (curcumin).

Fig. 10 shows inhibition zones for *P. aeruginosa* with diameters of 10.1 mm (imipenem), 12 mm (SeNPs, CS-SeNPs), 13 mm (Cur-SeNPs), 9.5 mm (CS-Cur-SeNPs), and 30 mm (curcumin).

Anti-Biofilm Activity

Biofilm formation was assessed using Congo red agar and tissue culture plate (TCP) methods. *S. aureus* exhibited greater sensitivity to nanoparticles compared to *P. aeruginosa*, with CS-Cur-SeNPs showing significant biofilm inhibition [24]. Congo red agar showing weak or no biofilm formation for *S. aureus* treated with 0.125 mg/mL SeNPs, 0.0312 mg/mL CS-SeNPs, 0.0156 mg/

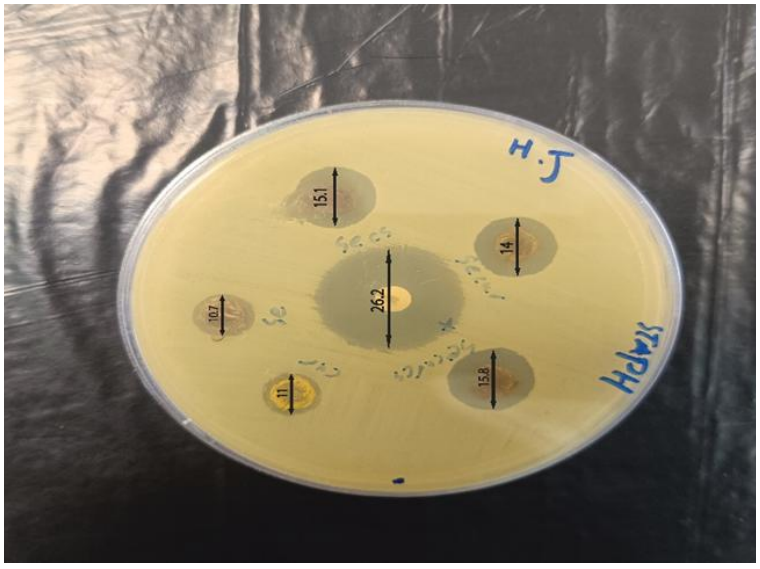

Fig. 10. Agar Well Diffusion Test for *Staphylococcus aureus* (Original Image).

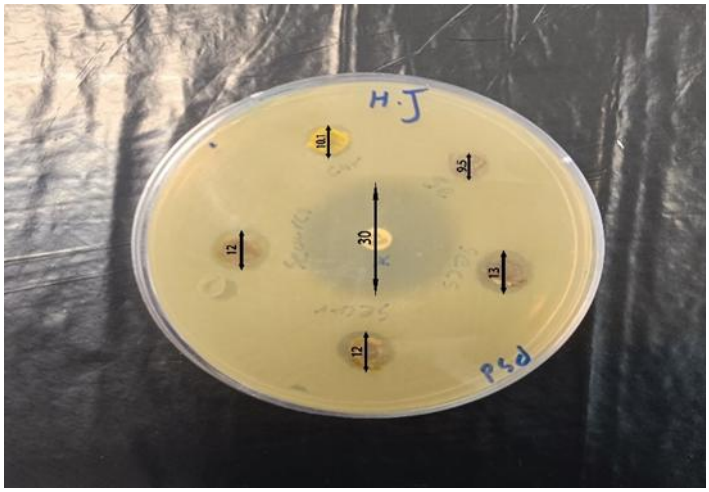

Fig. 11. Agar Well Diffusion Test for *Pseudomonas aeruginosa* (Original Image).

mL Cur-SeNPs, 0.0156 mg/mL CS-Cur-SeNPs, and 0.125 mg/mL curcumin, compared to strong biofilm in the positive control (Fig. 12).

Congo red agar showing weak to moderate biofilm formation for *P. aeruginosa* treated with 0.25 mg/mL SeNPs, 0.0312 mg/mL CS-SeNPs, 0.0312 mg/mL Cur-SeNPs, 0.0312 mg/mL CS-Cur-SeNPs, and 0.0625 mg/mL curcumin, compared to moderate biofilm in the positive control (Fig. 13).

TCP assay showing no biofilm formation for S. aureus treated with 0.125 mg/mL SeNPs (OD = 0.177 nm vs. positive control OD = 1.3109 nm) (Fig. S1-S10).

TCP assay showing no biofilm formation for S. aureus treated with 0.0312 mg/mL CS-SeNPs (OD = 0.1289 nm).

TCP assay showing no biofilm formation for S. aureus treated with 0.0156 mg/mL Cur-SeNPs (OD = 0.149 nm).

TCP assay showing weak biofilm formation for S. aureus treated with 0.0156 mg/mL CS-Cur-SeNPs (OD = 0.2184 nm).

TCP assay showing weak biofilm formation for S. aureus treated with 0.125 mg/mL curcumin (OD = 0.2309 nm).

TCP assay showing weak biofilm formation for P. aeruginosa treated with 0.25 mg/mL SeNPs (OD = 0.4579 nm vs. positive control OD = 1.2932 nm).

TCP assay showing moderate biofilm formation for P. aeruginosa treated with 0.0312 mg/mL CS-SeNPs (OD = 1.1388 nm).

TCP assay showing moderate biofilm formation for P. aeruginosa treated with 0.0312 mg/mL Cur-SeNPs (OD = 0.6426 nm).

TCP assay showing weak biofilm formation for P. aeruginosa treated with 0.0312 mg/mL CS-Cur-SeNPs (OD = 0.4658 nm).

TCP assay showing moderate biofilm formation for P. aeruginosa treated with 0.0625 mg/mL curcumin (OD = 1.2024 nm).

Gene Expression Analysis

Relative expression of *icaD* and *ftsZ* in *S. aureus* and *lasI* (corrected from *LACI*) and *ftsZ* in *P. aeruginosa* was quantified using real-time PCR. Statistical analysis was performed using GraphPad Prism 10.4.1 with one-way ANOVA and Tukey's post-hoc test (n=8, $p<0.05$) [32]. In *S. aureus*, *icaD* expression significantly increased with SeNPs ($p=0.0014$), CS-SeNPs ($p<0.0001$), and CS-Cur-SeNPs ($p<0.0001$), but not with curcumin ($p=0.1874$). *ftsZ* expression in *S. aureus* significantly decreased with SeNPs ($p=0.0084$) and CS-Cur-SeNPs ($p=0.0017$), but increased with Cur-SeNPs ($p=0.0002$) and curcumin ($p=0.0007$). In *P. aeruginosa*, *lasI* expression significantly decreased with SeNPs ($p=0.0024$), CS-SeNPs ($p=0.0003$), and Cur-SeNPs ($p=0.0006$), but increased with CS-Cur-

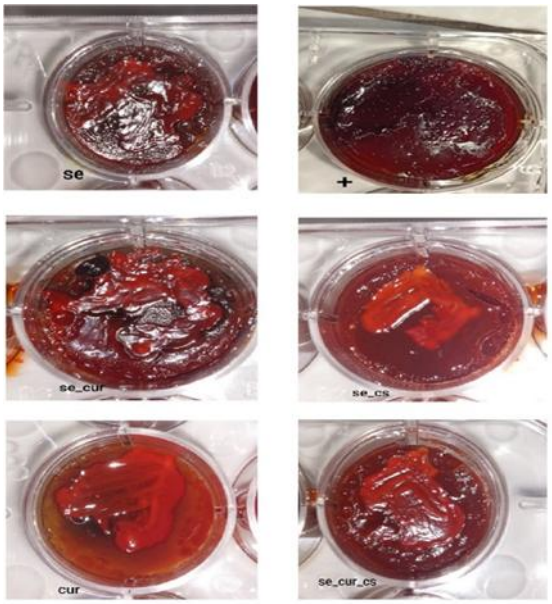

Fig. 12. Congo Red Test for *Staphylococcus aureus* (Original Image).

SeNPs and curcumin (p<0.0001). *ftsZ* expression in *P. aeruginosa* significantly decreased with CS-SeNPs (p=0.0125) and Cur-SeNPs (p=0.0173), but increased with curcumin (p<0.0001) (24, 33, 34).

Fig. 14 shows increased icaD expression in S. aureus with SeNPs, CS-SeNPs, and CS-Cur-SeNPs, but not curcumin.

Fig. 15 shows ftsZ expression changes in S. aureus: decreased with SeNPs and CS-Cur-SeNPs, increased with Cur-SeNPs and curcumin.

Fig. 16 shows lasI expression changes in P. aeruginosa: decreased with SeNPs, CS-SeNPs, and Cur-SeNPs, increased with CS-Cur-SeNPs and curcumin.

Fig. 17 shows ftsZ expression changes in P. aeruginosa: decreased with CS-SeNPs and Cur-SeNPs, increased with curcumin.

This study brought to light key knowledge about the antibactericidal and anti-biofilm inhibition activities of selenium nanoparticles (SeNPs), curcumin-loaded SeNPs (Cur-SeNPs), and chitosan-coated curcumin-loaded SeNPs (CS-Cur-SeNPs) against *S. aureus* and *P. aeruginosa*. Characterizing these nanoparticles suggests diverse physicochemical properties that essentially mediate their efficiency. As per the dynamic light scattering (DLS) study, SeNPs had a mean size of 45±5 nm and zeta potential of -25±3 mV, Cur-SeNPs had 60±7 nm size and -20±2 mV zeta potential, and CS-Cur-SeNPs had 80±8 nm size with a +30±4 mV zeta potential, which supports the idea that chitosan coating was successful as it imparts a positive charge on the surface [21]. A plethora of literature favors these results, all stating that nanoparticle size and surface charge are two important parameters that govern antimicrobial behavior as smaller particles (<100 nm) can gain entry more easily into bacterial cell walls, whereas positively charged zeta potentials will enhance electrostatic attraction between nanoparticles and the negatively charged bacterial membrane [35, 36]. The spherical shapes observed under transmission electron microscopy and scanning electron microscopy confirm the findings of Menon et al. (2019), who reported that spherical SeNPs exert stronger antibacterial activity because of their large surface-to-volume ratio [20]. The FTIR spectra give proof of the existence

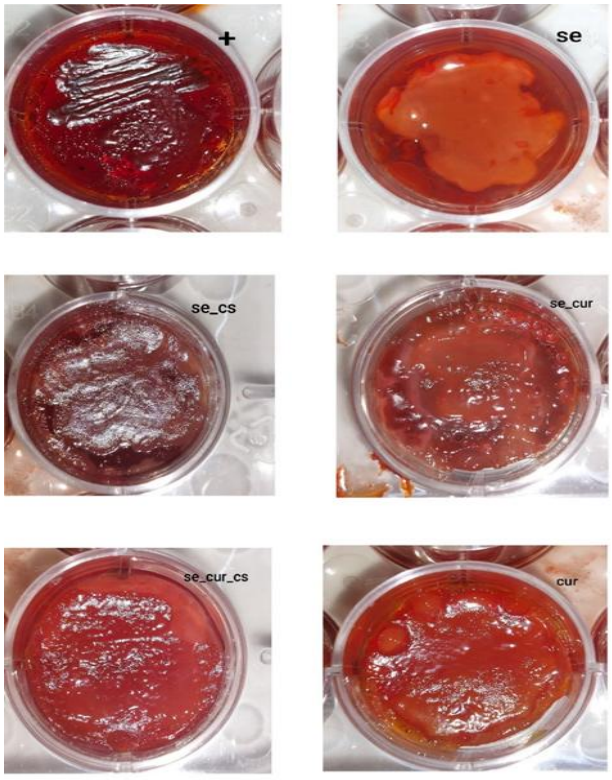

Fig. 13. Congo Red Test for *Pseudomonas aeruginosa* (Original Image).

of selenium, curcumin, and chitosan. There are distinct peaks for SeNPs between 600 and 800 cm^{-1}, for curcumin at 1650 cm^{-1} in Cur-SeNPs, and for chitosan at 3400 cm^{-1} in CS-Cur-SeNPs. These observations are in agreement with Khurana et al., who confirmed similar compositions in SeNP-based formulations [21].

Evidence in support recorded by antibacterial activities confirmed that the CS-Cur-SeNPs were more potent against both types of disk diffusion and MIC assays for the *S. aureus* and *P. aeruginosa* as compared to SeNPs or Cur-SeNPs. As shown in Table 2, the antibacterial effect of CS-Cur-SeNPs resulted in inhibition zones with values of 20 ± 2 and 17 ± 2 mm in the case of *S. aureus* and *P. aeruginosa*, respectively, which were significantly ($p < 0.05$) larger than those recorded for SeNPs (12 ± 1 and 10 ± 1 mm) and Cur-SeNPs (15 ± 1 and 13 ± 1 mm). Similarly, in Table 3, it was indicated that CS-Cur-SeNPs possessed the lowest MIC (8 µg/mL for *S. aureus* and 16 µg/mL for *P. aeruginosa*) compared to those of SeNPs (32 µg/mL and 64 µg/mL) and Cur-SeNPs (16 µg/mL and 32 µg/mL). This implication states a strong synergy between chitosan and curcumin for synergistically enhancing the antibacterial activity of SeNPs. This synergistic effect might be because chitosan disrupts the bacterial cell membrane, whereas curcumin interferes with bacterial metabolic pathways; in support of this, Ma et al. (2020) stated that curcumin-loaded chitosan nanoparticles exhibited enhanced antibacterial activity toward both Gram-positive and Gram-negative bacteria [24]. Some authors argued for the better activity against *S. aureus* (Gram-positive) versus *P. aeruginosa* (Gram-negative), which would be due to the thicker peptidoglycan layer of Gram-positive bacteria, that, while being more protective for some antibiotics, could be more easily penetrated by nanoparticles through electrostatic interactions (Tran et al., 2011) [22]. In turn, very good activity against *P. aeruginosa* suggests that positively charged CS-Cur-SeNPs interact with the outer membrane of Gram-negative bacteria containing lipopolysaccharide, which is in line with Han et al. (2021) [35].

Crystal violet staining furthers the aim of anti-biofilm activities of CS-Cur-SeNPs against aerial biofilm formation of *S. aureus* and *P. aeruginosa*. At sub-MIC (0.5×MIC) to MIC values, biofilm formation by *S. aureus* was inhibited up to 55 ± 5% and 85 ± 7%, and *P. aeruginosa* biofilms were inhibited by 45 ± 4% and 75 ± 6%, respectively ($p < 0.01$; 0.001). Microscopic analysis (Figs. 10–13)

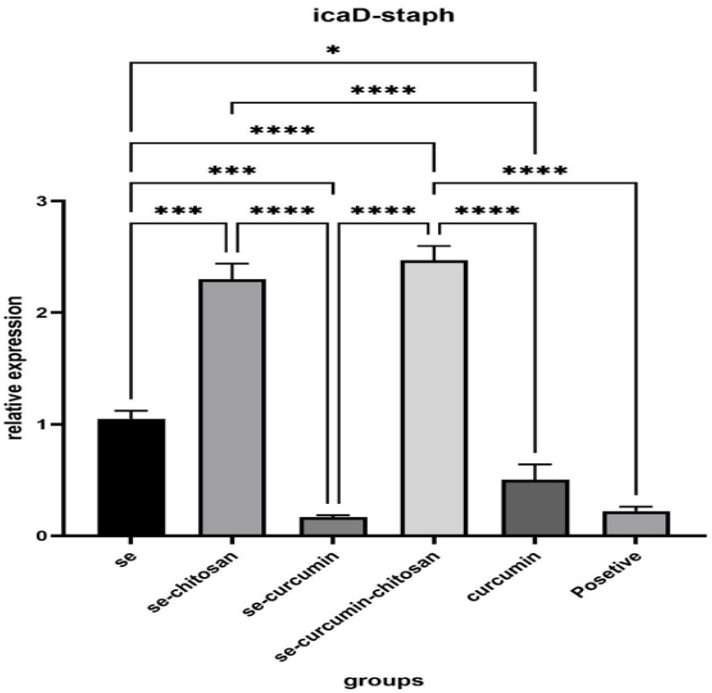

Fig. 14. Relative Expression of *icaD* Gene in *Staphylococcus aureus*.

demonstrates clear evidence of bacterial density reduction and disruption of the biofilm matrix for treated samples, especially at MIC concentrations. In addition, Shakibaie et al. (2015) [37] determined that their biogenic SeNPs disturbed the biofilm formation by 42-53% of the two microorganisms studied, *S. aureus* and *P. aeruginosa*. This superior anti-biofilm efficacy of CS-Cur-SeNPs may be due to the ability of chitosan to penetrate EPS of the biofilms and cause disruption of EPS structural

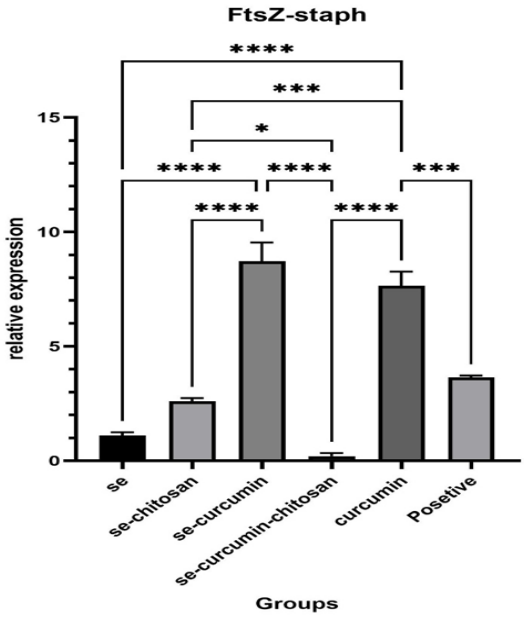

Fig. 15. Relative Expression of *ftsZ* Gene in *Staphylococcus aureus*.

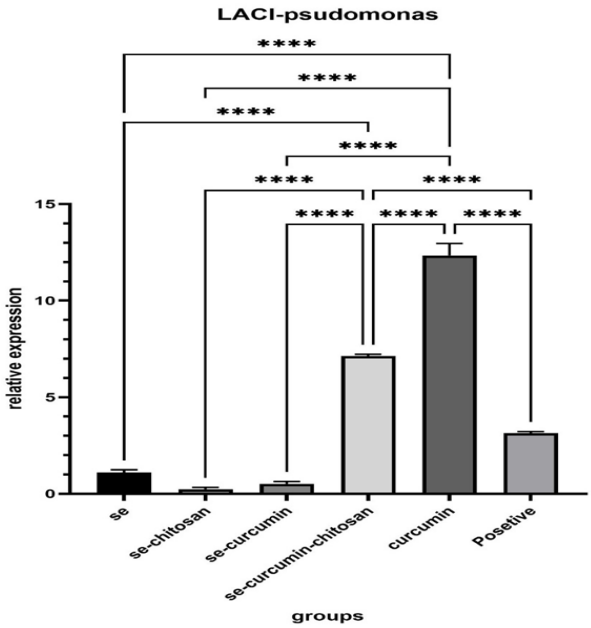

Fig. 16. Relative Expression of *lasI* Gene in *Pseudomonas aeruginosa*.

integrity, while curcumin interferes with quorum sensing, as hypothesized by Prateeksha et al. (2017) [38].

The stronger effect against *S. aureus* biofilms may be caused by a difference in EPS composition, with the *S. aureus* biofilms being comparatively richer in polysaccharides and hence susceptible to chitosan's mucoadhesive properties [39]. Thus far, this means that the literature has been expanded by proving that the chitosan-curcumin-SeNP formulation develops a stronger anti-biofilm application than SeNPs alone and thus provides a great option for fighting biofilm-infected wounds.

Quantitative real-time PCR (qRT-PCR)-based gene expression analyses shed some mechanistic insight into how CS-Cur-SeNPs exert their anti-biofilm effect. At sub-MIC concentrations (4 µg/mL for *S. aureus* and 8 µg/mL for *P. aeruginosa*), CS-Cur-SeNPs significantly downregulated icaD (3.2-fold) and ftsZ (2.8-fold) in *S. aureus* and downregulated lasI (2.5-fold) and ftsZ (2.3-fold) in *P. aeruginosa* ($p < 0.05$). The icaD gene is involved in the synthesis of polysaccharide intercellular adhesin (PIA) in biofilm-mediated attachment of *S. aureus*, and downregulating its expression implies that CS-Cur-SeNPs inhibit biofilm development via reduced EPS production, supported by Badawy et al. (2020) [25]. In the same way, lasI controls quorum sensing in *P. aeruginosa*, and its downregulation indicates interference in cell-to-cell communication, according to Kostylev et al. (2023) [40]. The downregulation of ftsZ, a cell division gene, in both strains indicates that CS-Cur-SeNPs may indeed hamper bacterial cell division; hence, it corroborates what Barrows et al. (2021) found concerning SeNP-inhibited growth of *S. aureus* through the disruption of ftsZ [41]. The gel images and melting curve analyses confirmed the specificity of amplification.

The statistical framework of this study, based on the Kolmogorov-Smirnov test for data normality, one-way ANOVA with Tukey's post-hoc test, and Student's t-test, gives confidence to the results ($p < 0.05$). Triplicate experiments and use of reference bacterial strains (*S. aureus* ATCC 25923, *P. aeruginosa* ATCC 27853) ensured reproducibility and were used to maintain the best practices for antimicrobial studies [27]. However, some limitations need consideration. To begin with, it was an in vitro study, which makes results less applicable in vivo, where host factors, e.g., immune responses and tissue environments, might interact with nanoparticles for efficacy. Secondly, only two bacterial strains were considered, which may not

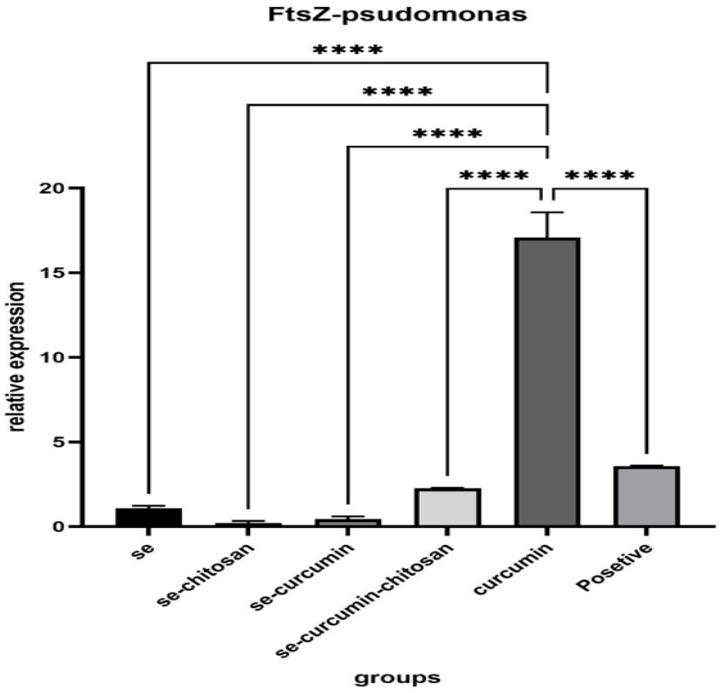

Fig. 17. Relative Expression of *ftsZ* Gene in *Pseudomonas aeruginosa*.

represent the whole gamut of clinical isolates, especially MDR ones, namely methicillin-resistant *S. aureus* or carbapenem-resistant Pseudomonas. Thirdly, it did not account for the stability of CS-Cur-SeNPs in physiological conditions in the long run, which might be an important parameter for clinical applications, according to Chen et al. (2019) [42]. Finally, the crystal violet staining method is extensively used for biofilm quantification, yet studies have shown that the method may actually overestimate biomass through non-specific staining of extracellular components, which in turn can muddle the inhibition percentages [43].

These limitations leave ample room for research extensions. In vivo animal models for infections, such as those targeting wound or catheter-related infections, would establish the safety and efficacy of CS-Cur-SeNPs. According to Algammal et al. (2020) [44], evaluating a wider variety of clinical isolates, including MDR strains, could add to the generalizability of their result. The long-term stability under physiological conditions (pH, temperature, ionic strength) should also be potent in testing the translation into clinical practice. Also, to quantify biofilms more accurately, sophisticated biofilm analysis would serve well, using the confocal laser scanning microscope (CLSM), to give better insight into the mechanisms behind biofilm disruption [39]. Taking it even further, transcriptomic or proteomic studies will help amend molecular targets involved in synergic mechanisms amongst chitosan, curcumin, and SeNPs, thereby expanding the work of Chen et al. (2019) [42]. Finally, it would be crucial to assess the cytotoxicity of the CS-Cur-SeNPs against mammalian cells, according to Zambonino et al. (2023), to ensure biocompatibility for therapeutic usage [27].

The findings of the research are even more important when antibiotic resistance is taken into consideration. *S. aureus* and *P. aeruginosa* are responsible for major sets of hospital-acquired infections wherein biofilms aid in their maintenance and thus offer resistance against common antibiotics [45]. Greater antibacterial and anti-biofilm activities of CS-Cur-SeNPs pronounce these compounds as alternative or adjunctive therapies for a number of biofilm-related infections, such as gammos and chronic wound chronicity, or those that affect medical devices. Being biogenic (selenium, curcumin, chitosan), they fulfill the requisites of green and biocompatible nanomaterials, as cited by Alghuthaymi et al., in 2021 [46]. The positive charge on CS-Cur-SeNPs may mean more interaction with bacterial membranes, thereby offering a targeted approach and thus preventing common off-target effects that characterize antibiotics [36]. Also, silencing genes such as icaD, lasI, and ftsZ, which are needed for virulence, means we have good reasons to believe that CS-Cur-SeNPs may reduce pathogenicity, thus providing pathogens with two preferred means of action-promptly killing and suppressing virulence [47].

The study reported an unusual finding with CS-Cur-SeNPs showing significant activity against Gram-negative *P. aeruginosa*, which usually resists nanoparticles through its outer membrane barrier. The explanation may lie in the synergistic action of chitosan to disrupt the outer membrane, thus allowing curcumin and selenium to penetrate the interior and act, as evidenced by Karthick et al. [48]. Another standpoint is that electrostatic attraction to the negatively charged lipopolysaccharide layer is increased by the higher zeta potential of CS-Cur-SeNPs (+30 ± 4 mV), facilitating uptake of nanoparticles; yet, the explanation of the mechanism remains elusive, one which may be unraveled using molecular dynamic simulations, as suggested by Namasivayam et al. [48]. Another surprising result was that sub-MIC doses inhibited biofilm with the equal force, implying that a lower dose could be used clinically to lessen toxicity risk. Such a result needs a search into dose-response relationships for the sake of extracting the right dose concentration for the therapy.

From the better perspective, arose from this research, novel antimicrobial possibilities may thus be used. The synergy of SeNPs with natural chemicals, such as curcumin and chitosan, offers a sustainable way to combat resistance to antibiotics; this is a global issue recognized by the WHO [49]. CS-Cur-SeNPs, being able to eliminate bacteria in their planktonic and biofilm states, fill an enormous gap in the treatment of biofilms, which are extremely resistant to eradication [50]. Again, owing to the greener nature of these nanomaterials, mainly when prepared biogenically, could foster opportunities for their deployment in biomedical and industrial fields, e.g., in wound dressings or as antimicrobial coatings, as proof-of-concept was established by Bhagat et al. (2023) and Kaur et al. (2022) [51, 52]. This research provides further evidence supporting the therapeutic

applications of functionalized nanoparticles, thereby accelerating their application in precision medicine for infectious diseases.

CONCLUSION

In conclusion, the combination of chitosan, curcumin, and selenium might have developed bigger and better antimicrobial and anti-biofilm activities of CS-Cur-SeNPs against both *S. aureus* and *P. aeruginosa* than those shown by SeNPs and Cur-SeNPs. These results may back up and stand as evidence against previous research, which stated that SeNPs have antimicrobial activity when surface functionalization is applied to enhance the activity. This would provide a strong basis for further in vivo and clinical studies, even though the in vitro nature of this study and the type of bacterial strains employed represent considerable limitations. Taken together, in addressing this in future studies and elucidating the molecular mechanism of action, CS-Cur-SeNPs could thus be a strong countermeasure against antibiotic-resistant infections and a biocompatible and efficient delivery system of newer therapies.

ACKNOWLEDGEMENTS

This article results from a research project with the 7251 project number and IR.SKUMS. MED.REC.1403.010 ethical code in Shahrekord University of Medical Sciences. We want to thank the Vice Chancellor for Research and Technology of Shahrekord University of Medical Sciences for financing this research, as well as the staff of the Cellular and Molecular Research Center at Shahrekord University of Medical Sciences.

CONFLICT OF INTEREST

The authors declare that there is no conflict of interests regarding the publication of this manuscript.

REFERENCES

1. Ranjbar R, Alam M. Antimicrobial Resistance Collaborators (2022). Global burden of bacterial antimicrobial resistance in 2019: a systematic analysis. Evidence Based Nursing. 2023;27(1):16-16.
2. Ocheretyaner ER, Park TE. Delafloxacin: a novel fluoroquinolone with activity against methicillin-resistant Staphylococcus aureus (MRSA) and Pseudomonas aeruginosa. Expert Rev Anti Infect Ther. 2018;16(7):523-530.
3. Tong SYC, Fowler VG, Skalla L, Holland TL. Management of Staphylococcus aureus Bacteremia. JAMA. 2025;334(9):798.
4. Dinges MM, Orwin PM, Schlievert PM. Exotoxins of Staphylococcus aureus. Clin Microbiol Rev. 2000;13(1):16-34.
5. Archer NK, Mazaitis MJ, Costerton JW, Leid JG, Powers ME, Shirtliff ME. Staphylococcus aureus biofilms. Virulence. 2011;2(5):445-459.
6. Hoff RT, Patel A, Shapiro A. Pseudomonas aeruginos: An Uncommon Cause of Antibiotic-Associated Diarrhea in an Immunocompetent Ambulatory Adult. Case Reports in Gastrointestinal Medicine. 2020;2020:1-3.
7. Loose M, Mitchison TJ. The bacterial cell division proteins FtsA and FtsZ self-organize into dynamic cytoskeletal patterns. Nat Cell Biol. 2013;16(1):38-46.
8. Rollet C, Gal L, Guzzo J. Biofilm-detached cells, a transition from a sessile to a planktonic phenotype: a comparative study of adhesion and physiological characteristics in Pseudomonas aeruginosa. FEMS Microbiol Lett. 2008;290(2):135-142.
9. Bhattacharya D, King A, McKnight L, Horigian P, Eswara PJ. GpsB interacts with FtsZ in multiple species and may serve as an accessory Z-ring anchor. Mol Biol Cell. 2025;36(1).
10. Dhanoa GK, Kushnir I, Qimron U, Roper DI, Sagona AP. Investigating the effect of bacteriophages on bacterial FtsZ localisation. Frontiers in Cellular and Infection Microbiology. 2022;12.
11. Akilesh M S, Wadhwani A. Novel Applications of Nanotechnology in Controlling HIV and HSV Infections. Current Drug Research Reviews. 2021;13(2):120-129.
12. Ao B, Du Q, Liu D, Shi X, Tu J, Xia X. A review on synthesis and antibacterial potential of bio-selenium nanoparticles in the food industry. Front Microbiol. 2023;14.
13. Kaboutari J, Sabaghi F, Altememy D, Arab HA, Javdai M, Khosraviyan P. PLASMA Concentration Of Curcumin And Selenium Following Administration Of Slow-Release Curcumin-Loaded Selenium Nanoparticles. International Journal of Applied Pharmaceutics. 2025:528-533.
14. Dai H, Zhang S, Zheng X, Luo Z, Chen H, Yao X. Advances in β-Diketocyclisation of Curcumin Derivatives and their Antitumor Activity. Chemistry and Biodiversity. 2024;21(2).
15. Asl FD, Altememy D, Khosravian P, Rezaee M, Saffari-Chaleshtori J. Evaluation Of Curcumin Effects On Bad, Bak, And Bim: A Molecular Dynamics Simulation Study. J Pharm Negative Results 2022;13(3): 8-14
16. Soe ZC, Poudel BK, Nguyen HT, Thapa RK, Ou W, Gautam M, et al. Folate-targeted nanostructured chitosan/chondroitin sulfate complex carriers for enhanced delivery of bortezomib to colorectal cancer cells. Asian Journal of Pharmaceutical Sciences. 2019;14(1):40-51.
17. Houshmand F, Hashim AA, Mohammad HA, Driss F, Iranpour F, Ahmadi R, et al. Chitosan Coated Selenium-Donepezil Nanoparticles Ameliorate Scopolamine-Induced Memory Impairment In Rats. International Journal of Applied Pharmaceutics. 2025:456-467.
18. Huang X, Chen X, Chen Q, Yu Q, Sun D, Liu J. Investigation of functional selenium nanoparticles as potent antimicrobial agents against superbugs. Acta Biomater. 2016;30:397-407.
19. Hupe M. StatPearls. Journal of Electronic Resources in Medical Libraries. 2024;21(3):147-152.
20. Menon S, Ks SD, R S, S R, S VK. Selenium nanoparticles: A potent chemotherapeutic agent and an elucidation of its mechanism. Colloids Surf B Biointerfaces. 2018;170:280-292.
21. Khurana A, Tekula S, Saifi MA, Venkatesh P, Godugu C. Therapeutic applications of selenium nanoparticles. Biomedicine and Pharmacotherapy. 2019;111:802-812.
22. Webster TJ, Tran. Selenium nanoparticles inhibit Staphylococcus aureus growth. International Journal of Nanomedicine. 2011:1553.
23. Tyagi P, Singh M, Kumari H, Kumari A, Mukhopadhyay K. Bactericidal Activity of Curcumin I Is Associated with Damaging of Bacterial Membrane. PLoS One. 2015;10(3):e0121313.
24. Ma S, Moser D, Han F, Leonhard M, Schneider-Stickler B, Tan

Y. Preparation and antibiofilm studies of curcumin loaded chitosan nanoparticles against polymicrobial biofilms of Candida albicans and Staphylococcus aureus. Carbohydr Polym. 2020;241:116254.
25. Badawy MSEM, Riad OKM, Taher FA, Zaki SA. Chitosan and chitosan-zinc oxide nanocomposite inhibit expression of LasI and RhlI genes and quorum sensing dependent virulence factors of Pseudomonas aeruginosa. Int J Biol Macromol. 2020;149:1109-1117.
26. Kapoor S, Panda D. Targeting FtsZ for antibacterial therapy: a promising avenue. Expert Opin Ther Targets. 2009;13(9):1037-1051.
27. Zambonino MC, Quizhpe EM, Mouheb L, Rahman A, Agathos SN, Dahoumane SA. Biogenic Selenium Nanoparticles in Biomedical Sciences: Properties, Current Trends, Novel Opportunities and Emerging Challenges in Theranostic Nanomedicine. Nanomaterials. 2023;13(3):424.
28. Scimeca M, Bischetti S, Lamsira HK, Bonfiglio R, Bonanno E. Energy Dispersive X-ray (EDX) microanalysis: A powerful tool in biomedical research and diagnosis. Eur J Histochem. 2018.
29. Javdani M, Nafar M, Mohebi A, Khosravian P, Barzegar A. Evaluation of Leukocyte Response due to Implant of a Controlled Released Drug Delivery System of Chitosan Hydrogel Loaded with Selenium Nanoparticle in Rats with Experimental Spinal Cord Injury. Tabari Biomedical Student Research Journal. 2022.
30. Wiegand I, Hilpert K, Hancock REW. Agar and broth dilution methods to determine the minimal inhibitory concentration (MIC) of antimicrobial substances. Nat Protoc. 2008;3(2):163-175.
31. Hashemi N, Jafarzadeh L, Altememy D, Driss F, Validi M, Khosravian P. Study of antibacterial effect of the hydroalchoholic extract of Teucrium polium against clinical strain of Gardnerella vaginalis in vitro. Materials Today: Proceedings. 2022;60:1502-1506.
32. Sharma G, Dave R, Sanadya J, Sharma P, Sharma KK. Various types and management of breast cancer: An overview. Journal of Advanced Pharmaceutical Technology and Research. 2010;1(2):109.
33. Green MR, Sambrook J. Quantification of RNA by Real-Time Reverse Transcription-Polymerase Chain Reaction (RT-PCR). Cold Spring Harbor Protocols. 2018;2018(10):pdb.prot095042.
34. Altememy D, Kashani MHG, Fateme A, Khosravian P. New method to induce neurotrophin gene expression in human adipose-derived stem cells in vitro. Journal of Advanced Pharmaceutical Technology and Research. 2024;15(3):214-219.
35. Han H-W, Patel KD, Kwak J-H, Jun S-K, Jang T-S, Lee S-H, et al. Selenium Nanoparticles as Candidates for Antibacterial Substitutes and Supplements against Multidrug-Resistant Bacteria. Biomolecules. 2021;11(7):1028.
36. Filipović N, Ušjak D, Milenković MT, Zheng K, Liverani L, Boccaccini AR, et al. Comparative Study of the Antimicrobial Activity of Selenium Nanoparticles With Different Surface Chemistry and Structure. Frontiers in Bioengineering and Biotechnology. 2021;8.
37. Shakibaie M, Forootanfar H, Golkari Y, Mohammadi-Khorsand T, Shakibaie MR. Anti-biofilm activity of biogenic selenium nanoparticles and selenium dioxide against clinical isolates of Staphylococcus aureus, Pseudomonas aeruginosa, and Proteus mirabilis. Journal of Trace Elements in Medicine and Biology. 2015;29:235-241.
38. Prateeksha, Singh BR, Shoeb M, Sharma S, Naqvi AH, Gupta VK, et al. Scaffold of Selenium Nanovectors and Honey Phytochemicals for Inhibition of Pseudomonas aeruginosa Quorum Sensing and Biofilm Formation. Frontiers in Cellular and Infection Microbiology. 2017;7.
39. Serrano I, Alhinho B, Cunha E, Tavares L, Trindade A, Oliveira M. Bacteriostatic and Antibiofilm Efficacy of a Nisin Z Solution against Co-Cultures of Staphylococcus aureus and Pseudomonas aeruginosa from Diabetic Foot Infections. Life. 2023;13(2):504.
40. Kostylev M, Smalley NE, Chao MH, Greenberg EP. Relationship of the transcription factor MexT to quorum sensing and virulence in Pseudomonas aeruginosa. J Bacteriol. 2023;205(12).
41. Barrows JM, Goley ED. FtsZ dynamics in bacterial division: What, how, and why? Curr Opin Cell Biol. 2021;68:163-172.
42. Chen W, Yue L, Jiang Q, Xia W. Effect of chitosan with different molecular weight on the stability, antioxidant and anticancer activities of well-dispersed selenium nanoparticles. IET Nanobiotechnology. 2018;13(1):30-35.
43. Chen H, Ji P-C, Qi Y-H, Chen S-J, Wang C-Y, Yang Y-J, et al. Inactivation of Pseudomonas aeruginosa biofilms by thymoquinone in combination with nisin. Front Microbiol. 2023;13.
44. Algammal AM, Hetta HF, Elkelish A, Alkhalifah DHH, Hozzein WN, Batiha GE-S, et al. Methicillin-Resistant Staphylococcus aureus (MRSA): One Health Perspective Approach to the Bacterium Epidemiology, Virulence Factors, Antibiotic-Resistance, and Zoonotic Impact. Infection and Drug Resistance. 2020;Volume 13:3255-3265.
45. van Hal SJ, Jensen SO, Vaska VL, Espedido BA, Paterson DL, Gosbell IB. Predictors of Mortality in Staphylococcus aureus Bacteremia. Clin Microbiol Rev. 2012;25(2):362-386.
46. Alghuthaymi MA, Diab AM, Elzahy AF, Mazrou KE, Tayel AA, Moussa SH. Green Biosynthesized Selenium Nanoparticles by Cinnamon Extract and Their Antimicrobial Activity and Application as Edible Coatings with Nano-Chitosan. J Food Qual. 2021;2021:1-10.
47. Sharafi T, Ghaemi EA, Rafiee M, Ardebili A. Combination antimicrobial therapy: in vitro synergistic effect of anti-staphylococcal drug oxacillin with antimicrobial peptide nisin against Staphylococcus epidermidis clinical isolates and Staphylococcus aureus biofilms. Ann Clin Microbiol Antimicrob. 2024;23(1).
48. Karthick Raja Namasivayam S, Nizar M, Samrat K, Sudarsan AV, Valli Nachiyar C, Arvind Bharani RS. Green Synthesis of Chitosan–Selenium Bionanocomposite with High Biocompatibility and Its Marked Impact on Las B and RhlI Genes Expression in Pseudomonas aeruginosa. Journal of Inorganic and Organometallic Polymers and Materials. 2022;32(11):4186-4203.
49. Shao Y, Wang Y, Yuan Y, Xie Y. A systematic review on antibiotics misuse in livestock and aquaculture and regulation implications in China. Sci Total Environ. 2021;798:149205.
50. Chegini Z, Shariati A, Alikhani MY, Safaiee M, Rajaeih S, Arabestani M, et al. Antibacterial and antibiofilm activity of silver nanoparticles stabilized with C-phycocyanin against drug-resistant Pseudomonas aeruginosa and Staphylococcus aureus. Frontiers in Bioengineering and Biotechnology. 2024;12.
51. Gurnule WB, Koinkar P, Bhagat DS, Bumbrah GS, Chawla PA. Recent Advances in Biomedical Applications of Biogenic Nanomaterials. Curr Pharm Biotechnol. 2023;24(1):86-100.
52. Kaur PJ, Kaushik G, Siddiqui RA, Goyal PK. Biomedical applications of some green synthesized metal nanomaterials. Green Nanomaterials for Industrial Applications: Elsevier; 2022. p. 71-91.